



ChemComm

3-ethyl-6-vinyltetrahydro-2H-pyran-2-one (EVP): A Versatile CO₂-Derived Lactone Platform for Polymer Synthesis

Journal:	<i>ChemComm</i>
Manuscript ID	CC-FEA-06-2022-003516.R1
Article Type:	Feature Article

SCHOLARONE™
Manuscripts

COMMUNICATION

3-ethyl-6-vinyltetrahydro-2H-pyran-2-one (EVP): A Versatile CO₂-Derived Lactone Platform for Polymer Synthesis

Rachel M. Rapagnani^a and Ian A. Tonks^{*, a}

Received 00th January 20xx,
Accepted 00th January 20xx

DOI: 10.1039/x0xx00000x

3-ethyl-6-vinyltetrahydro-2H-pyran-2-one (EVP) is a CO₂-derived lactone synthesized via Pd-catalyzed telomerization of butadiene. As EVP is 28.9% by weight CO₂, it has received significant recent attention as an intermediary for the synthesis of high CO₂-content polymers. This article provides an overview of strategies for the polymerization of EVP to a wide variety of polymer structures, ranging from radical polymerizations to ring-opening polymerizations, that each take unique advantage of the highly functionalized lactone.

As societal plastic production and use continues to increase at an enormous pace, there is an imperative need to develop sustainable materials that leverage waste products or renewable resources.^{1–4} Given their scale of production, it is also critical that new materials are potentially cost-competitive with current petroleum-based plastics. In this regard, the polymerization of CO₂ and alkenes is an important target in the context of a circular carbon economy:⁵ CO₂ is a waste product of the energy sector, and alkenes are inexpensive and abundant. However, the direct incorporation of CO₂ into polymers derived from commodity alkenes to create aliphatic polyesters has been a longstanding challenge in the field, precluded in part by the thermodynamic stability of CO₂.⁶

In the last eight years, the lactone 3-ethyl-6-vinyltetrahydro-2H-pyran-2-one (EVP)[†] has emerged as an intermediary that can bypass many of the challenges associated with the direct polymerization of CO₂ and alkenes. EVP is synthesized *via* the telomerization of butadiene with CO₂, a reaction which was discovered by Inoue⁷ and Musco⁸ in the 1970s (Figure 1, top). Butadiene is an inexpensive commodity chemical produced on an annual scale around 16 million tons (as of 2018),⁹ making it an ideal target cofeed for applications in cost-competitive CO₂-based materials.^{10,11} Further, butadiene can be synthesized from bio-based ethanol or butanediol,^{12,13} improving the longer-term sustainability profile of EVP-based materials.⁴

Since its discovery, the catalytic synthesis of EVP was heavily studied by Behr and Braunstein,¹⁴ and even more recently Beller,¹⁵ Bayón,¹⁶ and Bao^{17,18} have reported improved catalyst systems which have significantly increased the yield and selectivity of the reaction.

EVP can also be synthesized on a mini-plant scale, suggesting that the telomerization could be scaled up even further for wider industrial use, especially considering the scale of current industrial production of butadiene.^{10,11}

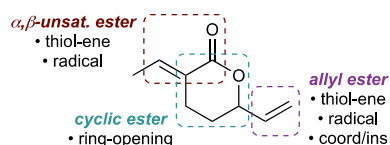
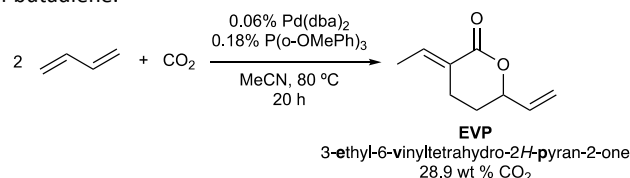


Figure 1. Top: Pd-catalyzed synthesis of EVP via butadiene/CO₂ telomerization. Bottom: functional group map of EVP describing polymerization strategies that have leveraged each group.

There are several features of EVP that make it an attractive target for polymerization, in addition to its inherently high CO₂ content (Figure 1, bottom). EVP is a cyclic ester, which can often be used in ring-opening polymerization (ROP);¹⁹ it contains an α,β-unsaturated ester, which can undergo radical polymerization; and finally, it is multifunctional (2 alkenes, 1 ester), which could be used for polyaddition reactions or post-polymerization modifications. Despite these attractive features, there are also several aspects of EVP that make it a challenging polymerization target. For example, multisubstituted α,β-unsaturated esters are often unreactive in radical polymerizations due to steric hindrance.^{20,21} Additionally, there are significant entropic penalties associated with the ring-opening of substituted lactones, which could render ring-opening polymerization of a disubstituted lactone such as EVP thermodynamically unfavorable.^{22,23} Finally, the α,β-unsaturation of the lactone could further render EVP susceptible to 1,4 Michael-type addition by nucleophiles rather than ester attack that would be needed for ring-opening polymerization. In fact, several reports detailed that EVP polymerization did not proceed with standard cationic, radical, or anionic initiators.^{24–27}

^aUniversity of Minnesota – Twin Cities
207 Pleasant St SE, Minneapolis, MN 55455

Although the first report of **EVP** copolymerization was reported in 1998,²⁴ the field was underdeveloped until the mid-to-late 2010s. New development has been spurred by a reassessment of the thermodynamic and kinetic viability of **EVP** in homo- and copolymerizations,²⁸ as well as increased motivation for incorporating CO₂ into sustainable and/or biodegradable materials.^{29,30} In this review, emerging strategies for **EVP** polymerization (polyaddition, radical, coordination/insertion, and ring-opening polymerization) will be highlighted.

Polyaddition of **EVP** via thiol-ene reactions

The first examples of **EVP** polymerization were polyaddition-type thiol-ene reactions that could take advantage of the reactivity of both double bonds in **EVP** (Figure 2). The first instance of **EVP** polyaddition copolymerization was reported by Dinjus in 1998, where successive thiol-ene click reactions of dithiols (2,2'-(ethylenedioxy)diethanethiol or 1,3-bis(3-meraptopropyl)-1,3,3-tetramethyldisiloxane) with both the allylic alkene and the α,β -unsaturated ester in **EVP** yielded moderate molar mass poly(**EVP-*alt*-dithiol**) polymers that maintained the cyclic lactone in the polymer backbone (Figure 2A). Initial reactivity studies with octylthiol revealed that the allylic alkene and the α,β -unsaturated ester of **EVP** each had similar rates of reactivity toward the addition of thiol radicals, which allowed for the productive AA+BB-like step growth polymerization. Although the lactone ring structure was maintained within the chain, the polymers displayed low glass transition temperatures ($T_g = -38$ °C to -35 °C).

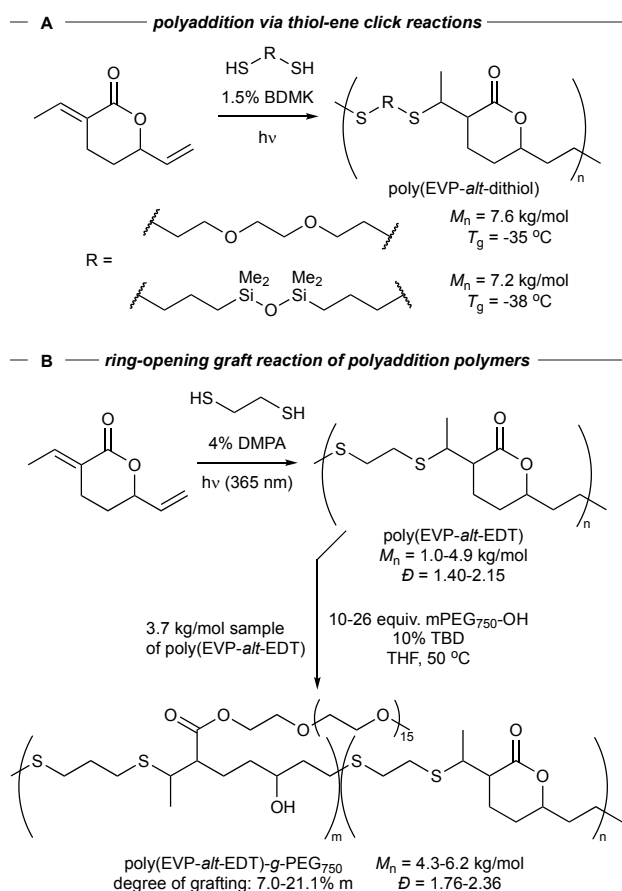


Figure 2. A: Initial examples of polyaddition of **EVP** via thiol-ene click reactions with various dithiol linkers. BDMK = benzildimethylketal. **B:** Post-polymerization grafting of polyethers to poly(**EVP-*alt*-EDT**) via TBD-catalyzed ring-opening. DMPA = 2,2-dimethoxy-2-phenylacetophenone. TBD = 1,5,7-triazabicyclo[4.4.0]decene.

In a recent report, Ni and Ling³¹ demonstrated that poly(**EVP-*alt*-EDT**) (**EDT** = ethylene dithiol) polymers synthesized *via* thiol-ene polyaddition could undergo post-polymerization modification through a ring-opening graft reaction with methoxy polyethylene glycol (mPEG-OH) (Figure 2B). In this instance, the ring-opening of the lactone was enabled by the loss of the α,β -unsaturation of the ester during the polymerization reaction, which makes ring-opening more facile.

Molar masses of the initial poly(**EVP-*alt*-EDT**) polyaddition polymers were modest (M_n up to 3.9 kg/mol). In this instance, an *in situ* NMR spectroscopic study revealed that the isolated double bond of the allylic ester moiety underwent thiol-ene reaction at about twice the rate of the α,β -unsaturated ester. This rate imbalance likely impedes molar mass growth of the step growth polymerization and also results in polymers whose end groups are primarily α,β -unsaturated esters.

Conveniently, the polyaddition/graft sequence could be carried out in a 1-pot, 2-step manner to directly generate amphiphilic graft copolymers. The glass transition temperature of the initial poly(**EVP-*alt*-EDT**) polymer was 24.5 °C, and after grafting with poly(ethylene glycol) methyl ether ($M_n = 750$ kg/mol) the T_g decreased to -37.1 °C. The resulting amphiphilic polymers could self-assemble into micelles with an average diameter of 98 nm.

Network polymers of **EVP** were also synthesized through thiol-ene reactions with pentaerythritol-tetrakis(3-mercaptopropionate).²⁴ The resulting network polymers were then used to make films of varying elasticity that displayed swelling behavior.

Additionally, photoinitiated crosslinking of **EVP** with tri(ethylene glycol)dithiol (TEGDT) and/or trimethylolpropane tris(3-mercaptopropionate) (TMPT) forms networks with variable thermal and tensile properties depending on the loadings of each crosslinker.³² Higher TMPT content compared to TEGDT increases the T_g (up to 20 °C), decomposition temperature (up to 333 °C), Young's modulus (up to 9.6 MPa), and tensile strength (up to 6.18 MPa), and decreases the strain at break (down to 1.39 mm/mm). The 50:50 TEGDT:TMPT network was further complexed with various metal ions, Cu²⁺, Ni²⁺, Fe³⁺, and Co²⁺, increasing the T_g from 3.4 °C to 22.9 °C, and increasing the tensile strength from 2.1 MPa up to 3.3 MPa. These networks displayed fluorescence under UV light and could be used for photopatterning.

Radical (co)polymerization of **EVP** and **EVP** derivatives

The first successful homopolymerization of **EVP** was demonstrated in a landmark report in 2014 by Nozaki *via* radical polymerization (Figure 3).³³ Initiation of the polymerization with the azo radical initiator V-40 (V-40 = 1,1'-azobis(cyclohexane-1-carbonitrile)) resulted in radical addition on the allylic ester of **EVP** followed by cyclization across the lactone, resulting in a polymer ($M_n = 5.7$ kg/mol, $D = 1.3$) containing exclusively a bicyclic lactone repeat unit (α). Conditions for reversible deactivation radical polymerization (nitroxide-mediated or atom-transfer radical polymerization) did not initiate polymerization. This bicyclic lactone polymer was later shown to undergo reversible post-polymerization modification through lactone ring-opening by hydrolysis or aminolysis.³⁴

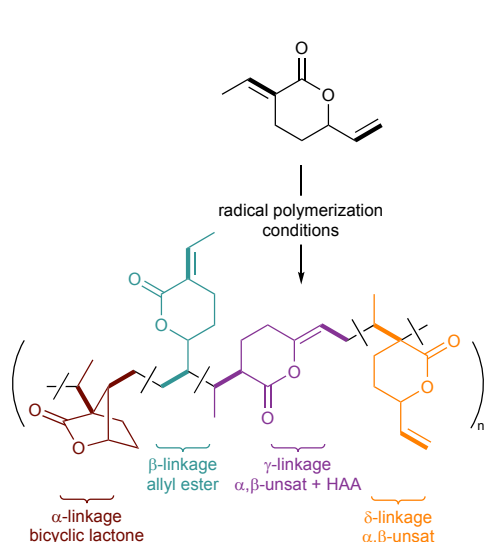


Figure 3. Radical polymerizations of **EVP** demonstrating that initiation conditions and additives dramatically impact the radical linkage structures and M_n . EC = ethylene carbonate.

Addition of a Lewis acidic additive ($ZnCl_2$) and solvent (ethylene carbonate) during **EVP** radical polymerization dramatically increased the molar mass of the resulting polymer ($M_n = 85$ kg/mol, $D = 1.5$), but also introduced two additional structures into the polymer backbone (β and γ) as a consequence of differential radical propagation: allylic ester radical polymerization without cyclization (β) or tiglate radical formation/intramolecular H atom abstraction (HAA) (γ). This high molar mass polymer had a high glass transition temperature ($T_g = 192$ °C) owing to the rigid bicyclic backbone. Lin later established that radical polymerization of **EVP** could be thermally initiated by O_2 in air, reaching M_n values up to 239 kg/mol with T_g values of 111–129 °C.³⁵ Radical polymerization under these conditions produced an additional repeat unit structure (δ) resulting from direct chain propagation from the tiglate unit without cyclization or HAA.

Similar CO_2 /diene copolymers could also be synthesized via a 1-pot, 2-step telomerization/polymerization sequence, which allowed for the incorporation of isoprene or piperylene into the polymer framework (Figure 4). Successful homotelomerizations of isoprene³⁶ or piperylene with CO_2 have not been reported, so cotelomerizations with butadiene followed by *in situ* polymerization of the resulting lactone products were undertaken. For example, reaction of piperylene in a 2:1 ratio with butadiene predominantly led to a single lactone product **1** from the heterocoupling of 1 piperylene with 1 butadiene, which could then be polymerized analogously to **EVP**.

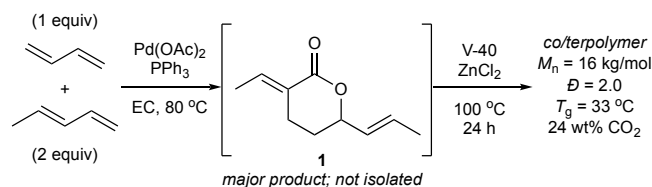


Figure 4. One-pot cotelomerization and subsequent radical polymerization provides a route to incorporate isoprene or piperylene (shown) into CO_2 -based materials.

Radical copolymerizations of **EVP** have also been reported (Figure 5). For example, **EVP** can undergo azobisisobutyronitrile (AIBN)-initiated radical copolymerization with ethylene to yield low molar mass ($M_n = 1.3$ to 3.8 kg/mol) functionalized polyethylene with 0.53% - 6.8 mol% of incorporated **EVP**.³⁷ In this radical copolymerization, both the allylic ester and α,β -unsaturated ester moieties were reactive, forming exclusively bicyclic lactone units along the main chain (type α). Interestingly, increasing the amount of **EVP** in the reaction decreased the copolymer molar mass, because the stability of the α -carbonyl radical that is generated upon radical addition to the α,β -unsaturated ester impedes chain growth. As in the case of the **EVP** bicyclic lactone homopolymer³⁴, the bicyclic backbone moiety can undergo post-polymerization modification through ring-opening aminolysis of the ester.

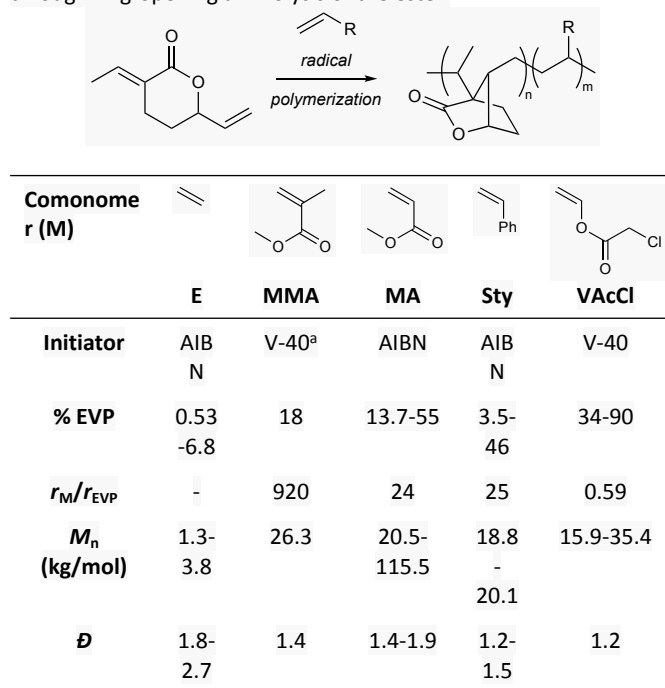


Figure 5. Radical copolymerizations of **EVP**. ^aSlow addition of MMA was performed to keep f_{MMA} low.

EVP also undergoes radical copolymerization with methyl methacrylate, methyl acrylate, styrene, vinyl chloroacetate, and vinyl acetate to give high molar mass bicyclic lactone copolymers with varying degrees of **EVP** incorporation (13–90 mol% **EVP**) (Figure 5).³⁸ In most cases **EVP** undergoes slower incorporation into the growing polymer chain compared to the vinyl monomer ($r_{MMA/EVP} = 920$; $r_{MA/EVP} = 24$; $r_{Sty/EVP} = 25$), with the exception of vinyl chloroacetate ($r_{VAcCl/EVP} = 0.6$). The rigid bicyclic lactone units increased the T_g values of all of the vinyl copolymers: for example, poly(MMA-co-**EVP**) ($M_n =$

26.3 kg/mol, 18 mol% **EVP**) had a T_g of 126 °C, greater than atactic poly(MMA) ($T_g = 105$ °C).

In order to overcome the poor reactivity of **EVP** in radical polymerizations, Ni synthesized a methacrylate-appended **EVP** derivative, methyl-2-ethylidene-5-hydroxyhept-6-enoate methacrylate (**MEDMA**), through a 2-step methanolysis/acylation sequence (Figure 6).³⁹ Although **MEDMA** is a trivinyl monomer, reversible addition-fragmentation chain-transfer (RAFT) polymerization of **MEDMA** mediated by 2-cyanoprop-2-yl-dithiobenzoate (CPDB) yielded linear polymers that reacted solely through the methacrylate alkene (Figure 6, RAFT Cond. A). These linear-selective polymerizations provided precision control over molar mass with comparatively low dispersities. Interestingly, extended reaction times resulted in extremely high molar mass hyperbranched polymers ($M_w > 100$ kg/mol) resulting from reactivity from the **EVP** moiety of **MEDMA** (Figure 6, RAFT Cond. B). Model copolymerizations of MMA with *cis*-3-hexenyl tiglate (no incorporation) and allyl phenyl ether (some incorporation) led to the conclusion that hyperbranching in the **MEDMA** polymerizations is primarily a result of incorporation of the allyl ester group from **EVP** into the polymer backbone.

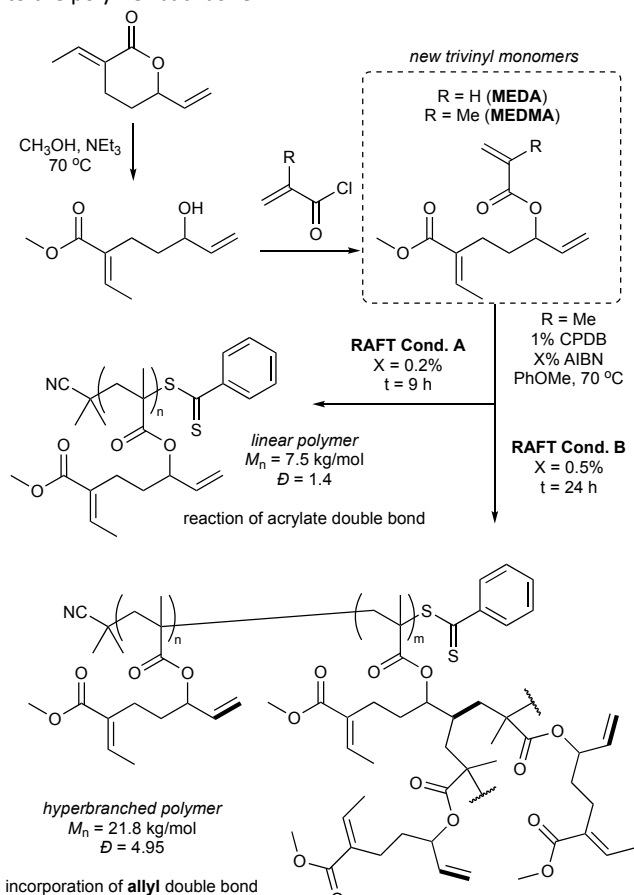


Figure 6. Synthesis of new trivinyl monomers **MEDA**/**MEDMA** and RAFT polymerization of **MEDMA** leading to either linear or hyperbranched polymers.

Coordination/insertion (co)polymerization of **EVP** and **EVP** derivatives

The allyl ester of **EVP** can be considered a functionalized α -olefin and thus could be copolymerized via coordination/insertion polymerization, although this type of copolymerization is often

difficult with polar functional alkenes.^{40,41} Nonetheless, Nozaki has demonstrated that **EVP** can undergo coordination/insertion copolymerization with ethylene catalyzed by Pd complexes, yielding lactone-appended polyethylenes.³⁷ In these instances, the coordination/insertion polymerization of **EVP** occurs solely through the allyl moiety, providing an orthogonal/complementary reactivity pattern and resultant microstructure compared to the radical copolymerizations of **EVP** and ethylene (*vide supra*). Pd complexes of both phosphine-sulfonate and carbene-phenolate ligands were active for the copolymerizations. In general, the carbene-phenolate catalysts provided higher incorporation ratios (0.47–3.7% vs. 0.04–0.32%) compared to the phosphine-sulfonate catalysts, albeit with lower activity (0.6–9.5 $\text{g}\cdot\text{mmol}^{-1}\cdot\text{h}^{-1}$ vs. 13–48 $\text{g}\cdot\text{mmol}^{-1}\cdot\text{h}^{-1}$). The resultant lactone-appended polyethylenes could also undergo post-polymerization functionalization via Michael addition of nitromethane to the α,β -unsaturated ester.

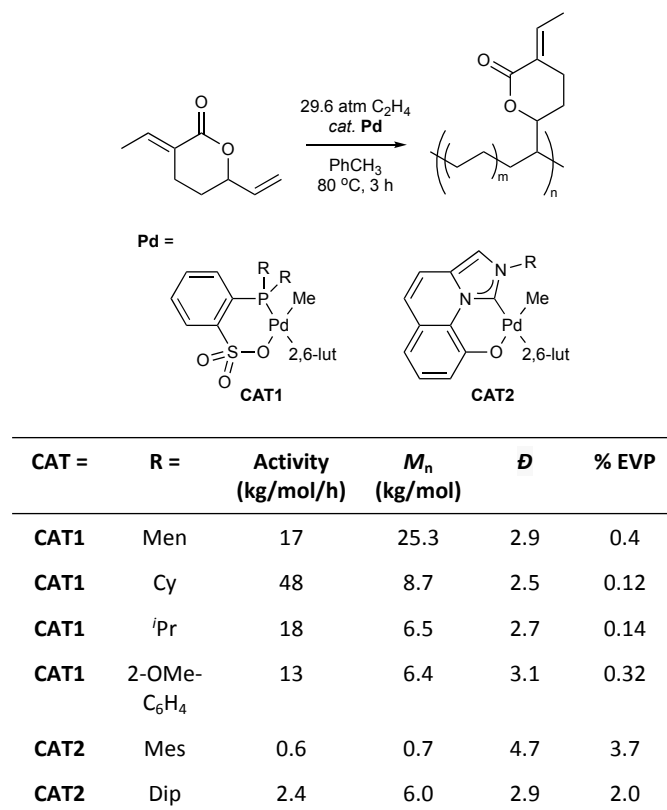
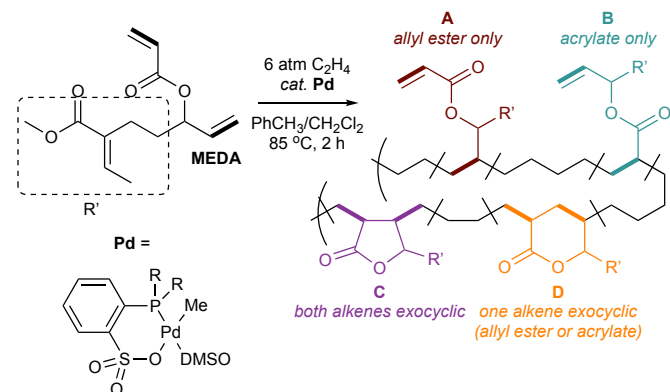


Figure 7. Pd-catalyzed coordination/insertion copolymerization of ethylene with **EVP**.

Ni also reported coordination/insertion copolymerization of an **EVP**-acrylate derivative **MEDA** (methyl-2-ethylidene-5-hydroxyhept-6-enoate acrylate, see Figure 6 for synthesis) with ethylene, which resulted in complex microstructures owing to the multiple reactive alkenes in **MEDA** (Figure 8).⁴² In these copolymerizations, Brookhart-type α -diimine Pd complexes were unable to incorporate **MEDA**. Building off of an example of cyclopolymerization of allyl acrylate,⁴³ it was discovered that phosphine-sulfonate Pd complexes could provide moderate incorporation (1.1–3.1%) of **MEDA** into polyethylene.



R =	Activity (kg/mol/h)	M_n (kg/mol)	\bar{D}	% EVP	A:B:C:D
2-OMe- C ₆ H ₄	7	8.8	2	1.3	5:16:71:9
Cy	7.5	10.7	2.1	1.1	9:40:43:9
2,4,6- (OMe) ₃ C ₆ H ₂ / ^t Bu	8	27.5	2.1	0.8	9:40:44:6

Figure 8. Copolymerization of the acrylate-type monomer **MEDA** with ethylene.

Microstructure analysis of the **MEDA**-incorporated polyethylenes revealed predominantly backbone cyclic lactones (C, D) with pendent α,β -unsaturated esters (40-70% of the **MEDA** units) that resulted from acrylate/allyl insertion/cyclization. Additionally, the polymers contained pendent acrylate side chains (A) resulting from allyl insertion (up to 11% of the **MEDA** units) and pendent allyl side chains (B) from acrylate insertion (up to 45%). No instances of α,β -unsaturated ester incorporation were detected. Conveniently, the ratios of the microstructures can be tuned by varying the steric bulk of the phosphine-sulfonate ligand of the catalyst.

Ring-opening (co)polymerization of **EVP** and **EVP** derivatives

There remain no reports of ring-opening homopolymerization of **EVP** to a polyester, though there are several accounts that detail failed **EVP** ring-opening polymerization.^{24,25,27} However, substantial progress in the last year has helped to better map the chemical landscape and challenges of **EVP** ring-opening polymerizations.

The first example of a ring-opening copolymerization with **EVP** was only reported in 2021, when Ni disclosed a $\text{Sc}(\text{OTf})_3$ -initiated cationic copolymerization of β -butyrolactone (BBL) with **EVP** (Figure 9).²⁷ The resulting poly(BBL-*r*-**EVP**) had low molar masses ($M_n = 0.5$ -1.1 kg/mol) and large dispersities ($\bar{D} = 1.9$ -3.7), owing to unavoidable chain transfer of the cationic chain ends. Nonetheless, this method allows for up to 50 mol% **EVP** incorporation into the copolymer.

Mass spectrometric analysis of the BBL/**EVP** copolymerization revealed a predominantly alternating character to the copolymerization, where there were virtually no **EVP** diads present. DFT calculations demonstrated that homopropagations of either **EVP** or BBL were not kinetically favored, as the BBL-onto-**EVP**-end (31.9 kcal/mol) and **EVP**-onto-BBL-end (25.4 kcal/mol) processes had lower ΔG^\ddagger values than **EVP**-onto-**EVP**-end (38.0 kcal/mol) or BBL-onto-BBL-end (30.4 kcal/mol). The reactivity ratios were determined

to be 0.01 for **EVP** and 0.27 for BBL, highlighting the significant difficulty of **EVP** ring-opening homopolymerization.

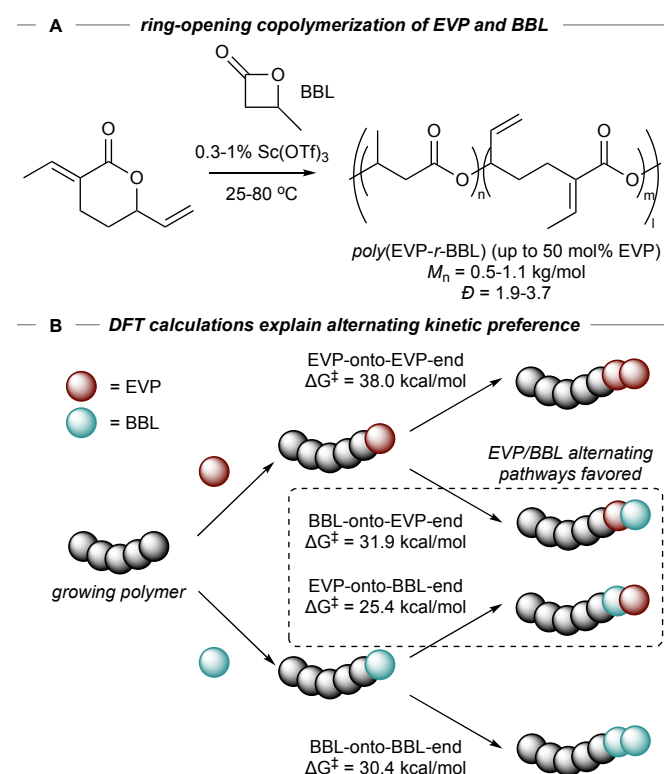


Figure 9. A: Ring-opening copolymerization of **EVP** with β -butyrolactone (BBL) using $\text{Sc}(\text{OTf})_3$. B: Gas-phase DFT calculations (M06-2X/6-31+G(d,p)) of the copolymerization demonstrate a preference for alternating behavior because of lower kinetic barriers to alternating ROP transition states.

Eagan⁴⁴ demonstrated that treatment of **EVP** with TBD/benzyl alcohol (TBD = 1,5,7-triazabicyclo[4.4.0]dec-5-ene) results in a high viscosity material with a ¹H NMR spectrum inconsistent with Ni's ring-opened²⁷ **EVP** microstructure. Detailed analysis revealed that **EVP** undergoes dimerization through vinylogous 1,4-Michael addition, and the resulting Michael product can undergo concurrent ring-opening polymerization (Figure 10). Because 1,4-Michael addition and ROP compete, low molar mass poly(**EVP**) brush-like polymers are generated where the average sidechain includes 2 **EVP** subunits that have undergone conjugate addition (x -avg = 2). MALDI-TOF (matrix-assisted laser desorption/ionization time-of-flight) mass spectrometry of the poly(**EVP**) samples shows TBD end groups, indicating that TBD is both catalyst and initiator, propagating through an acyl ammonium intermediate.

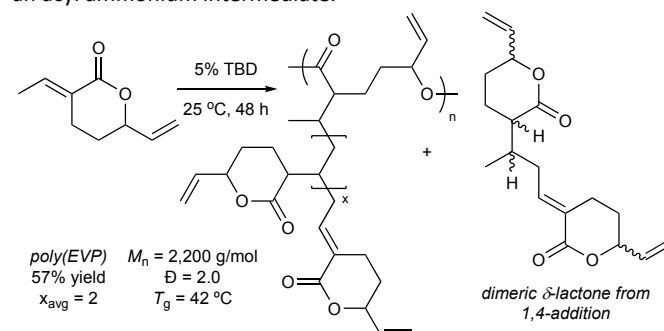


Figure 10. TBD-catalyzed polymerization of **EVP** results in a material produced from vinyllogous conjugate addition and subsequent ring-opening polymerization.

The propensity toward ring-opening of **EVP** analogues that do not have the α,β -unsaturated ester (as demonstrated in post-polymerization modifications reported by Nozaki³⁴ and the concurrent 1,4-addition polymerization reported by Eagan⁴⁴) indicate that it may be feasible to polymerize saturated **EVP** derivatives. In fact, two recent reports have demonstrated that the hydrogenated **EVP** derivatives 3-ethyl-6-vinyltetrahydro-2H-pyran-2-one (**EtVP**) and 3,6-diethyl-tetrahydro-2H-pyran-2-one (**DEP**) are viable monomers for ring-opening polymerization to polyesters. Both **EtVP** and **DEP** can be synthesized via high-yielding and simple reduction protocols (Figure 11A).^{45,46}

In the first example of ring-opening homopolymerization of an **EVP** derivative, we reported the polymerization of **EtVP** under neat conditions using the bifunctional base TBD⁴⁷ as a catalyst along with phenylpropanol (PPA) initiator (Figure 11B).⁴⁸ The resulting polymer had high molar mass and low dispersity ($M_n = 13.6$ kg/mol, $\mathcal{D} = 1.32$), and a low glass transition temperature (-39 °C) in line with other polyesters derived from substituted valerolactones.²² TBD is a much more effective catalyst for **EtVP** ROP ($k_{\text{obs}} = 1.44$ M/h) than diphenylphosphate ($k_{\text{obs}} = 0.029$ M/h), which is commonly used for ROP of other 6-membered lactones. Interestingly, TBD was not an effective catalyst for **DEP** ROP (46% conversion in 3 d); however, a NaOMe/1-cyclohexyl-3-phenylurea catalyst system polymerized **DEP** to high conversion (70%) with good molar mass and low dispersity ($M_n = 9.7$ kg/mol, $\mathcal{D} = 1.27$).

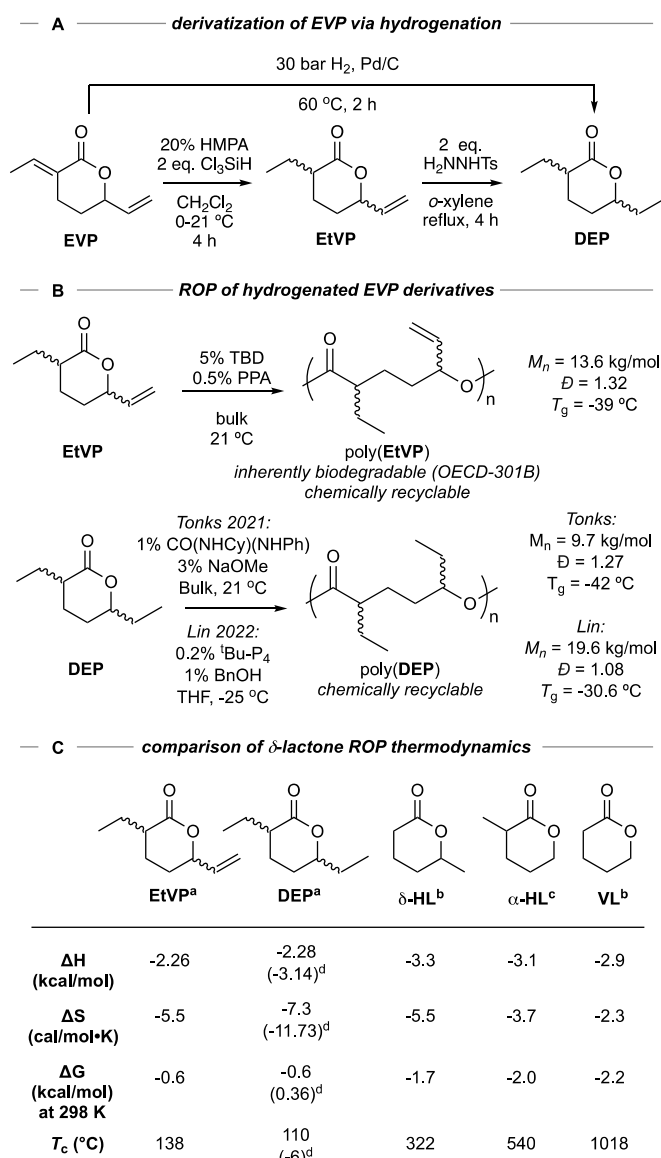


Figure 11. Ring-opening polymerization of reduced **EVP** derivatives. A: Selective hydrogenation of **EVP** to **EtVP** and exhaustive hydrogenation to **DEP**. B: First demonstrations of the ROP of **EtVP** and **DEP**. C: Thermodynamic parameters for the polymerization of **EtVP** and **DEP** compared to other δ -lactones. Data obtained from ^aref. 48; ^bref. 23; ^cref. 22; ^dref. 49.

van 't Hoff analysis of the **EtVP** and **DEP** polymerizations revealed that each were only slightly exergonic at room temperature (**EtVP**: $\Delta G = -0.6$ kcal/mol; **DEP**: $\Delta G = -0.6$ kcal/mol) and as a result have reasonably low ceiling temperatures ($T_c = 138$ °C for **EtVP**; 110 °C for **DEP**) (Figure 11C). As a result, poly(**EtVP**) can be chemically recycled by catalytic depolymerization and distillation at elevated temperature. Further, poly(**EtVP**) was shown to be biodegradable in wastewater (OECD-301B protocol). Several post-polymerization modifications of poly(**EtVP**) were also demonstrated, taking advantage of simple thiol-ene click reactions with the side chain vinyl group.

Shortly after this initial report, Lin reported a phosphazene base, ^tBu-P₄ (1-tert-butyl-4,4-tris(dimethylamino)-2,2-bis[tris(dimethylamino)phosphoranylide-namino]-2 λ^5 ,4 λ^5 -catenadi(phosphazene)), that was highly active for ROP of **DEP** to

poly(DEP).⁴⁹ More typical catalysts for ROP were initially employed, but either exhibited no reactivity (tin(II)2-ethylhexanoate, dibutyltin dilaurate, or diphenylphosphate) or underwent very slow polymerization with moderate conversion (TBD). The authors speculated that increasing the basicity may increase the reactivity, leading to the exploration of phosphazene bases and the discovery of the highly active ^tBu-P₄ catalyst (pK_a = 42.7). Polymerization of DEP with ^tBu-P₄/benzyl alcohol led to high molar mass polyester with low dispersity ($M_n = 19.6$ kg/mol, $\mathcal{D} = 1.08$). Initial mechanistic studies indicate an anionic polymerization mechanism. Notably, carboxylates are indicated as potentially dormant species that could be generated from adventitious water, which may explain why polymerizations of EtVP⁴⁸ and DEP are quite water sensitive, and also why previous attempts at DEP ROP had failed.

Interestingly, polymerizations with ^tBu-P₄ catalyst in the absence of initiator resulted in the formation of ultrahigh molar mass cyclic polymer ($M_n = 543$ -614 kg/mol, $\mathcal{D} = 1.35$ -1.45). The high molar mass cyclic poly(DEP) polymers showed pressure-sensitive adhesive properties comparable to commercial tapes from 3M® (peel strength = 0.015-0.038 N/m). The high molar mass cyclic poly(DEP) polymers can also be chemically recycled back to DEP with high mass recovery (up to 100%) through depolymerization with ZnCl₂ or (La[N(SiMe₃)₂]₃) at elevated temperature.

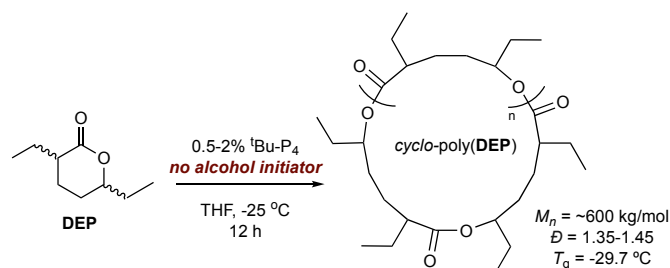


Figure 12. Ultrahigh molar mass cyclo-poly(DEP) can be synthesized using ^tBu-P₄ at -25 °C without the addition of an initiator.

Outlook

Recent years have demonstrated the promise of **EVP** as an intermediary for the incorporation of CO₂ into polymers, and strategies that leverage every functional group of **EVP** have yielded access to materials with diverse properties and degradation potential. Remarkably, **EVP** contains functional groups that on the surface appear challenging to polymerize (substituted α,β -unsaturated ester or the highly substituted lactone ring), yet creative applications of synthesis and catalysis are unlocking its potential across many different polymerization methods and materials classes. Given the density of functionality of **EVP** there remain significant opportunities to develop new polymerization strategies, and also to further implement catalysis to improve the nascent reports herein. Overall, the work presented here establishes a strong foundation for the synthesis of materials with high CO₂ content that, until recently, were thought to be inaccessible.

Acknowledgements

The funding for this work was provided by the NSF Center for Sustainable Polymers (CHE-1901635)

Author Contributions

I.A.T. and R.M.R. contributed equally to this article.

Notes and references

† There is some discrepancy in naming this lactone: EVL and EVP are both common in the literature. Here, we prefer EVP because P (pyranone) is more descriptive of the monomer structure than L (lactone).

- 1 D. K. Schneiderman and M. A. Hillmyer, *Macromolecules*, 2017, **50**, 3733–3749.
- 2 M. Hong and E. Y. X. Chen, *Trends Chem.*, 2019, **1**, 148–151.
- 3 Y. Zhu, C. Romain and C. K. Williams, *Nature*, 2016, **540**, 354–362.
- 4 D. E. Fagnani, J. L. Tami, G. Copley, M. N. Clemons, Y. D. Y. L. Getzler and A. J. McNeil, *ACS Macro Lett.*, 2021, **10**, 41–53.
- 5 World Economic Forum, Ellen MacArthur Foundation and McKinsey and Company, *The New Plastics Economy Rethinking the Future of Plastics*; 2016; [report] <http://www.ellenmacarthurfoundation.org/publications>.
- 6 C. J. Price, B. Jesse, E. Reich and S. A. Miller, *Macromolecules*, 2006, **39**, 2751–2756.
- 7 Y. Inoue, Y. Sasaki and H. Hashimoto, *Bull. Chem. Soc. Jpn.*, 1978, **51**, 2375–2378.
- 8 V. Musco, A., Perego, C., Tartari, *Inorganica Chim. Acta*, 1978, **28**, 147–148.
- 9 I. Bin Samsudin, H. Zhang, S. Jaenicke and G. K. Chuah, *Chem. - An Asian J.*, 2020, **15**, 4199–4214.
- 10 A. Behr and M. Heite, *Chem. Eng. Technol.*, 2000, **23**, 952–955.
- 11 A. Behr and M. Becker, *J. Chem. Soc. Dalt. Trans.*, 2006, 4607–4613.
- 12 E. V. Makshina, M. Dusselier, W. Janssens, J. Degréve, P. A. Jacobs and B. F. Sels, *Chem. Soc. Rev.*, 2014, **43**, 7917–7953.
- 13 D. Sun, Y. Li, C. Yang, Y. Su, Y. Yamada and S. Sato, *Fuel Process. Technol.*, 2020, **197**, 106193.
- 14 P. Braunstein, D. Matt and D. Nobel, *J. Am. Chem. Soc.*, 1988, **110**, 3207–3212.
- 15 M. Sharif, R. Jackstell, S. Dastgir, B. Al-Shihi and M. Beller, *ChemCatChem*, 2017, **9**, 542–546.
- 16 J. M. Balbino, J. Dupont and J. C. Bayón, *ChemCatChem*, 2018, **10**, 206–210.
- 17 J. Song, X. Feng, Y. Yamamoto, A. I. Almansour, N. Arumugam, R. S. Kumar and M. Bao, *Tetrahedron Lett.*, 2016, **57**, 3163–3166.
- 18 Y. Dai, X. Feng, B. Wang, R. He and M. Bao, *J. Organomet. Chem.*, 2012, **696**, 4309–4314.
- 19 N. E. Kamber, W. Jeong, R. M. Waymouth, R. C. Pratt, B. G. G. Lohmeijer and J. L. Hedrick, *Chem. Rev.*, 2007, **107**, 5813–5840.
- 20 M. L. Miller and J. Skogman, *J. Polym. Sci. Part A Gen. Pap.*, 1964, **2**, 4551–4558.
- 21 E. Kassi and C. S. Patrickios, *Macromolecules*, 2010, **43**, 1411.
- 22 D. K. Schneiderman and M. A. Hillmyer, *Macromolecules*, 2016, **49**, 2419–2428.
- 23 P. Olsén, K. Odelius and A. C. Albertsson,

- Biomacromolecules*, 2016, **17**, 699–709.
- 24 V. Haack, E. Dinjus and S. Pitter, *Angew. Makromol. Chemie*, 1998, **257**, 19–22.
- 25 V. Hardouin Duparc, R. M. Shakaroun, M. Slawinski, J. F. Carpentier and S. M. Guillaume, *Eur. Polym. J.*, 2020, **134**, 109858.
- 26 K. Nozaki, *Bull. Chem. Soc. Jpn.*, 2021, **94**, 984–988.
- 27 S. Yue, T. Bai, S. Xu, T. Shen, J. Ling and X. Ni, *ACS Macro Lett.*, 2021, **10**, 1055–1060.
- 28 S. Tang and K. Nozaki, *Acc. Chem. Res.*, 2022, **55**, 1524–1532.
- 29 B. Grignard, S. Gennen, C. Jérôme, A. W. Kleij and C. Detrembleur, *Chem. Soc. Rev.*, 2019, **48**, 4466–4514.
- 30 S. Dabral and T. Schaub, *Adv. Synth. Catal.*, 2019, **361**, 223–246.
- 31 J. Song, K. Chen, Y. Feng, X. Ni and J. Ling, *J. Polym. Sci.*, 2022, 1–10.
- 32 L. Chen, J. Ling, X. Ni and Z. Shen, *Macromol. Rapid Commun.*, 2018, **39**, 1–6.
- 33 R. Nakano, S. Ito and K. Nozaki, *Nat. Chem.*, 2014, **6**, 325–331.
- 34 S. Moon, K. Masada and K. Nozaki, *J. Am. Chem. Soc.*, 2019, **141**, 10938–10942.
- 35 M. Liu, Y. Sun, Y. Liang and B. L. Lin, *ACS Macro Lett.*, 2017, **6**, 1373–1378.
- 36 E. Dinjus and W. Leitner, *Appl. Organomet. Chem.*, 1995, **9**, 43–50.
- 37 S. Tang, Y. Zhao and K. Nozaki, *J. Am. Chem. Soc.*, 2021, **143**, 17953–17957.
- 38 M. R. Hill, S. Tang, K. Masada, Y. Hirooka and K. Nozaki, *Macromolecules*, 2022, **55**, 3311–3316.
- 39 L. Chen, Y. Li, S. Yue, J. Ling, X. Ni and Z. Shen, *Macromolecules*, 2017, **50**, 9598–9606.
- 40 A. Keyes, H. E. Basbug Alhan, E. Ordonez, U. Ha, D. B. Beezer, H. Dau, Y. S. Liu, E. Tsogtgerel, G. R. Jones and E. Harth, *Angew. Chemie - Int. Ed.*, 2019, **58**, 12370–12391.
- 41 C. Tan and C. Chen, *Angew. Chemie*, 2019, **131**, 7268–7276.
- 42 Y. Zhang, J. Xia, J. Song, J. Zhang, X. Ni and Z. Jian, *Macromolecules*, 2019, **52**, 2504–2512.
- 43 J.-C. Daigle, L. Piche, A. Arnold and J. P. Claverie, *ACS Macro Lett.*, 2012, **1**, 343–346.
- 44 L. D. G. Espinosa, K. Williams-Pavliantou, K. M. Turney, C. Wesdemiotis and J. M. Eagan, *ACS Macro Lett.*, 2021, **10**, 1254–1259.
- 45 M. Sugiura, N. Sato, S. Kotani and M. Nakajima, *Chem. Commun.*, 2008, **2**, 4309–4311.
- 46 A. Behr and V. A. Brehme, *J. Mol. Catal. A Chem.*, 2002, **187**, 69–80.
- 47 B. G. G. Lohmeijer, R. C. Pratt, F. Leibfarth, J. W. Logan, D. A. Long, A. P. Dove, F. Nederberg, J. Choi, C. Wade, R. M. Waymouth and J. L. Hedrick, *Macromolecules*, 2006, **39**, 8574–8583.
- 48 R. M. Rapagnani, R. J. Dunscomb, A. A. Fresh and I. A. Tonks, *Nat. Chem.* 2022, *In press* DOI:10.1038/s41557-022-00969-2.
- 49 Y. Lou, L. Xu, N. Gan, Y. Sun and B. L. Lin, *Innov.*, 2022, **3**, 100216.